Hydrothermal Synthesis of new Iodates $Ln_2(IO_3)_3(IO_4)$ (*Ln*=La, Nd, Pr) Containing the Tetraoxoiodate(V) Anion: Creation of Luminescence Properties by Doping with Eu, Dy, Tb

Ceren Kutahyali Aslani[a †], Vladislav V. Klepov[a], Mahmoud A. A. Aslani[b], and Hans-Conrad zur Loye[*a]

[a]Department of Chemistry and Biochemistry, University of South Carolina, Columbia, SC 29208, USA

[b]Department of Mechanical Engineering, University of South Carolina, Columbia, SC 29208, USA

*Corresponding author: zurloye@mailbox.sc.edu

†Current address: Los Alamos National Laboratory, Carlsbad Operations, Carlsbad, 88220 NM

Abstract

We report on the detailed structural analysis and luminescent properties of the novel iodates $Ln_2(IO_3)_3(IO_4)$ (*Ln*=La, Nd, Pr) obtained successfully via mild hydrothermal synthesis. The structures were determined by single crystal X-ray diffraction and the phase purity of the samples were established by powder X-ray diffraction. $Ln_2(IO_3)_3(IO_4)$ crystallizes in the orthorhombic crystal system adopting the *Pbca* space group. The complex structures contain the rare $[IO_4]^{3-}$ units. The band gaps of the materials were determined from UV-Vis data and optical band gaps were estimated to be 3.0 and 3.4 eV for $La_2(IO_3)_3(IO_4)$ and $Nd_2(IO_3)_3(IO_4)$, respectively. $La_2(IO_3)_3(IO_4)$ was used as a host matrix for Eu, Tb, and Dy doping to introduce luminescence.

Introduction

Iodate compounds continue to attract attention due to their interesting structures and their potential applications in the areas of nonlinear optics (NLO) [1], luminescence [2], and photocatalysis [3]. Iodates consisting of IO_3 and IO_4 groups, which create rich functional properties and display rich structural chemistry, have attracted widespread attention for many years,[4] especially when the structures contain $[IO_4]$ units, that impart even more structural complexity. The Albrecht-Schmitt group first reported on the tetraoxoiodate(V) $[IO_4]^{3-}$ species in $Ag_4(UO_2)_4(IO_3)_2(IO_4)_2O_2$ and $Ba[(MoO_2)_6(IO_4)_2O_4]\cdot H_2O$,[5,6] and it is present in some more complex iodates species.[7] According to their structural results the tetraoxoiodate(V) anion has a stereochemically active lone pair. Another structure containing $[IO_4]^{3-}$ species, $Bi_2(IO_4)(IO_3)_3$, was reported by Cao et al., who discussed the material as a new potential infrared (IR) nonlinear optical (NLO) material.[8] Iodates based on I^{5+} contain a lone pair and tend to form two types of coordination environments, that of $[IO_3]^-$ and $[IO_4]^{3-}$ units, assuming weak I-O interactions (>2.4 Å) are neglected [5,9,10,11]. Due to the presence of this stereochemically active lone pair, many metal iodates crystallize in noncentrosymmetric (NCS) structures, causing them to be extensively studied for their NLO properties.[12],[13] The combination of the stereochemically active lone pair on both the I^{5+} and the Bi^{3+} species, such as in $Bi_2(IO_4)(IO_3)_3$, favors NCS structures, as the addition of yet one more lone pair containing cation seems to favor NCS structures. [14-16]

A second interesting class of optical properties, luminescence, is observed in several rare earth cations and has prompted research into lanthanide containing materials in order to study the characteristic luminescence of the 4f to 4f electronic transitions.[17,18]. Rare earth containing iodates with their complex structural chemistry [19] can exhibit highly desired luminescence behavior, including long luminescence lifetimes, sharp emission bands, and a large energy gap between the absorption and emission bands.[20] Although luminescence is intrinsic to these specific lanthanides and incorporating them into new materials almost guarantees luminescence, the structure does impart its own modulation on the luminesce behavior, providing continued impetus to investigate lanthanide containing materials for their optical properties.

Herein we report on the synthesis and properties of a series a new rare earth based iodates, a class of promising luminescence materials. Using similar reaction conditions $Ln_2(IO_3)_3(IO_4)$ (*Ln*=La, Nd, Pr) were successfully crystallized. The structure contains the very

rare $[IO_4]^{3-}$ units that to date have been reported in only in a very small number of crystal structures. Unlike many of the known metal iodate structures, $Ln_2(IO_3)_3(IO_4)$ (*Ln*=La, Nd, Pr) crystallize in a centrosymmetric (CS) space groups, which precludes them from having second harmonic generation (SHG) response. To induce and study their luminescence behavior, $La_2(IO_3)_3(IO_4)$ was doped with Eu, Tb, Dy, and their luminescence behavior is reported as well.

EXPERIMENTAL

Reagents

La_2O_3 (Alfa Aesar, 99.99%), Pr_6O_{11} (Alfa Aesar, 99.99%), Nd_2O_3 (Alfa Aesar, 99.99%), Gd_2O_3 (Alfa Aesar, 99.99%), Tb_4O_7 (Alfa Aesar, 99.9%), Dy_2O_3 (Alfa Aesar, 99.9%), HIO_3 (Alfa Aesar, 99%) were all used as received.

Synthesis

For $La_2(IO_3)_3(IO_4)$, 0.326 g (1 mmol) of La_2O_3 and 0.528 g (3 mmol) of HIO_3 were combined with 5 mL of H_2O. For $Nd_2(IO_3)_3(IO_4)$, 0.337 g (1 mmol) of Nd_2O_3 and 0.528 g (3 mmol) of HIO_3 were combined with 5 mL of H_2O. For $Pr_2(IO_3)_3(IO_4)$, 0.512 g (0.5 mmol) of Pr_6O_{11} and 0.264 g (1.5 mmol) of HIO_3 were combined with 5 mL of H_2O. Each solution was placed in a 23-mL PTFE-lined autoclave that was subsequently sealed. The autoclaves were gradually heated to 220°C, held for 4 days, and cooled slowly to room temperature at a rate of 6°C h^{-1}. The products were recovered by filtration and washed with water. Pure colorless and purple crystals of $La_2(IO_3)_3(IO_4)$ and $Nd_2(IO_3)_3(IO_4)$ were obtained, respectively. Green $Pr_2(IO_3)_3(IO_4)$ crystals were also synthesized. Doped samples were synthesized using the same procedure, however, the quantify of the rare earth starting materials were reduced to 0.95 mmol and 0.05 mmol of Eu_2O_3, Dy_2O_3 or Tb_4O_7 were added as dopant.

Property Measurements and Characterization

Details regarding instrumentation and procedures for the single crystal structure determination, [21,22,23,24] powder diffraction measurements, elemental analysis, and optical measurements are provided in the SI.

Single Crystal X-ray Diffraction

Single-crystal X-ray diffraction data and results of the diffraction experiments are summarized in Table 1 and Table S1-S6.

Table 1. Crystallographic data for $Ln_2(IO_3)_3(IO_4)$ (*Ln*=La, Nd, Pr)

Chemical formula	$La_2(IO_3)_3(IO_4)$	$Nd_2(IO_3)_3(IO_4)$	$Pr_2(IO_3)_3(IO_4)$
Formula weight	993.42	1004.08	997.42
Crystal system	orthorhombic		
Space group, Z	*Pbca*		
a, Å	7.4460(2)	7.3459(2)	7.3701(2)
b, Å	13.9248(3)	13.7615(3)	13.7958(3)
c, Å	22.1286(5)	21.9824(6)	22.0267(5)
V, $Å^3$	2294.38(9)	2222.21(10)	2239.60(9)
ρ_{calcd}, g/cm^3	5.752	6.002	5.916
Radiation (λ, Å)	MoKα (0.71073)		
μ, mm^{-1}	18.181	20.427	19.697
T, K	302	293	299.91
Crystal dim., mm^3	0.04×0.02×0.02	0.06×0.06×0.05	0.20×0.05×0.05
2θ range, deg.	2.926-27.496	2.960-27.499	2.953- 36.354
Reflections collected	36172	30512	216600
Data/parameters/restraints	2637/173/0	2539/173/0	5434/173/0
R_{int}	0.0554	0.0381	0.0388
Goodness of fit	1.190	1.242	1.098
$R_1(I > 2\sigma(I))$	0.0233	0.0170	0.0155
wR_2(all data)	0.0416	0.0376	0.0329

RESULTS AND DISCUSSION

Synthesis

It is well known that lanthanum iodates crystallize in different polymorphs depending on the specific synthesis method employed: hydrothermal vs. evaporation.[2] Taouti et al. explored reactions with $[IO_3^-]$:$[La^{3+}]$ molar ratios equal to 10 and 5 by evaporation, which yielded the structures of $La(IO_3)_3(HIO_3)_{1.33}$ and $La(IO_3)_3(HIO_3)$, respectively. When they replaced the lanthanum reagent, $LaCl_3$, with La_2O_3, used an $[IO_3^-]$:$[La^{3+}]$ molar ratio of 4 and performed the synthesis via the hydrothermal method, α-$La(IO_3)_3$ crystals were obtained. Hector et al.[25,26] investigated the hydrothermal synthesis of iodates starting from the corresponding periodates, which resulted in $La(IO_3)_3$•$1/2H_2O$, $Sc(IO_3)_3$, and $Y(IO_3)_3$•$2H_2O$. They were able to extend the series by adjusting the heating parameters to yield $Lu(IO_3)_3$•$2H_2O$, $Ln(IO_3)_3$ (Ln = Pr, Nd, Sm, Eu, Gd, Tb, Ho, Er), and $Ln(IO_3)_3$•$2H_2O$ (Ln = Eu, Gd, Dy, Er, Tm, Yb).

To achieve the synthesis of crystals of the new lanthanide iodate title compounds, $Ln_2(IO_3)_3(IO_4)$, (*Ln* = La, Nd, Pr) we used a mild hydrothermal synthesis method adapted from that of Ok and Halasyamani [27] who used it to synthesize $La(IO_3)_3$. As mentioned above, many factors influence product formation and the quantities of HIO_3 and water used in the synthesis also have a strong effect on the product that crystallizes. Using a 5 times lower concentration of HIO_3 relative to conditions that result in $La(IO_3)_3$, we were able to crystallize $Ln_2(IO_3)_3(IO_4)$, *Ln*: La, Nd, Pr. Unlike $La(IO_3)_3$, which crystallizes in a non-centrosymmetric space group, $Ln_2(IO_3)_3(IO_4)$, *Ln*: La, Nd, Pr crystallize in a centrosymmetric orthorhombic space group. The synthesis of the praseodymium phase is more difficult as only the use of Pr_6O_{11} as the starting rare-earth oxide, rather than Pr_2O_3, results in $Pr_2(IO_3)_3(IO_4)$. Pr_2O_3 inevitably resulted in the previously reported $Pr(IO_3)_3$. Unfortunately, only very few crystals of $Pr_2(IO_3)_3(IO_4)$ formed, preventing the characterization of this phase beyond the structure determination. Interestingly, attempts to crystallize the later rare earths yielded $Ln(IO_3)_3$ (Gd, Tb, and Dy), which are known compositions, suggesting that the rare earth size also has an important effect on product formation and indicates that the $Ln_2(IO_3)_3(IO_4)$ structure requires the larger rare earth cations to form. This is consistent with the fact that Cao et al.[8] was able to synthesize $Bi_2(IO_3)_3(IO_4)$, structurally closely related, with $La_2(IO_3)_3(IO_4)$, containing Bi^{3+} which is slightly larger than La^{3+}. Also, this is consistent with our observations that there is often a change in the structure

that crystallizes as a function of rare earth size, for example in the $Cs_2NaLn(PS_4)_2$ [28] and the $CsLnP_2S_7$ [29] series.

The preparation of the Eu, Tb, Dy doped $La_2(IO_3)_3(IO_4)$ samples used the same synthesis route that yielded $La_2(IO_3)_3(IO_4)$, except that the starting reagents contained a 95% La_2O_3 and 5% Eu_2O_3, Tb_2O_3, Dy_2O_3, respectively. The doped samples were determined to be phase pure by powder X-ray diffraction and the diffraction pattern matches that of $La_2(IO_3)_3(IO_4)$. The presence of the dopants was confirmed by EDS in a semi-quantitively determined concentrations of 3.7, 1.8, and 5.4% for Eu, Dy, and Tb, respectively (Fig S3-S9 and Table S7).

Crystal Structure

$Ln_2(IO_3)_3(IO_4)$ crystallizes in a new structure type (Fig 1) in the centrosymmetric orthorhombic space group *Pbca*. The structure contains two Ln cations, four I atoms, and thirteen O atoms. The structure is closely related to that of $Bi_2(IO_4)(IO_3)_3$ which crystallizes in the non-centrosymmetric orthorhombic space group $P2_12_12_1$.[8] As shown in Figure 1a, $La_2(IO_4)(IO_3)_3$ has a three-dimensional (3D) framework structure composed of IO_3, IO_4, LaO_9, and LaO_{10} polyhedra (Fig 1 b-e). LaO_{10} polyhedra share edges with neighboring LaO_{10} polyhedra and each LaO_{10} polyhedron also shares faces and edges with two different LaO_9 polyhedra, while LaO_9 polyhedra share corners with their neighboring LaO_9 polyhedra to form La-O layers in which the La1 and La2 atoms are located in chains oriented along the y direction (Fig 1f). I2, I3, and I4 atoms, which connect to the La atoms via bridging oxygen atoms, are attached to these layers, while I1 atoms further join these layers together via bridging oxygen atoms to form the framework structure (Fig 1g).

The coordination environment of I1, I2, and I3, shown in Figure 1, is that of a trigonal pyramid. The three I−O distances range from 1.779(4) to 1.828(4) Å, which is in agreement with I-O distances reported for $La(IO_3)_3$ (1.781(13)−1.830(12) Å). [27] The lone pair is assumed to be located roughly opposite the I-O bonds. The coordination environment of I4 is best described as a seesaw, with I−O distances of 1.833(4)−1.988(4) Å, which are consistent with the I-O distances of 1.807(6)−2.102(6) Å found in $Bi_2(IO_4)(IO_3)_3$.[8] It is interesting to note that the IO_3 and IO_4 groups reported in the literature all connect with each other through O atoms to form

$[I_3O_8]^-$ anions [12,27,30,31]. In this new $La_2(IO_4)(IO_3)_3$ structure, the IO_3 and IO_4 groups are all isolated from each other and do not have a common O atom.

The coordination polyhedra of La1 and La2 cations are irregular with coordination numbers of 10 and 9 and La−O distances in the range of 2.411(4)−2.767(4) Å. These La-O distances are very similar those of 2.416(13)-2.834(12) Å in $La(IO_3)_3$.[2] All bond lengths and atomic coordinates are listed in Tables S1-S6 and PXRD patterns of compounds can be found in Figure S1 and S2 in the Supporting Information. The bond valence sums for all compounds were calculated and were found to be consistent with the 3+ oxidation state for the rare earths and the 5+ oxidation state for iodine. The individual results are listed in Table S8.

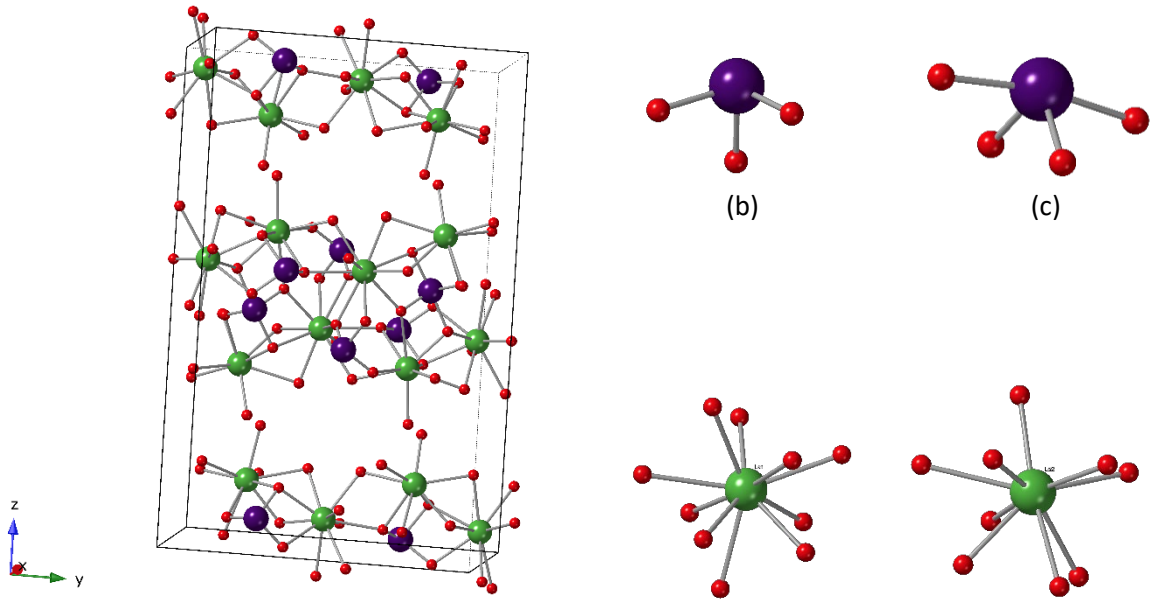

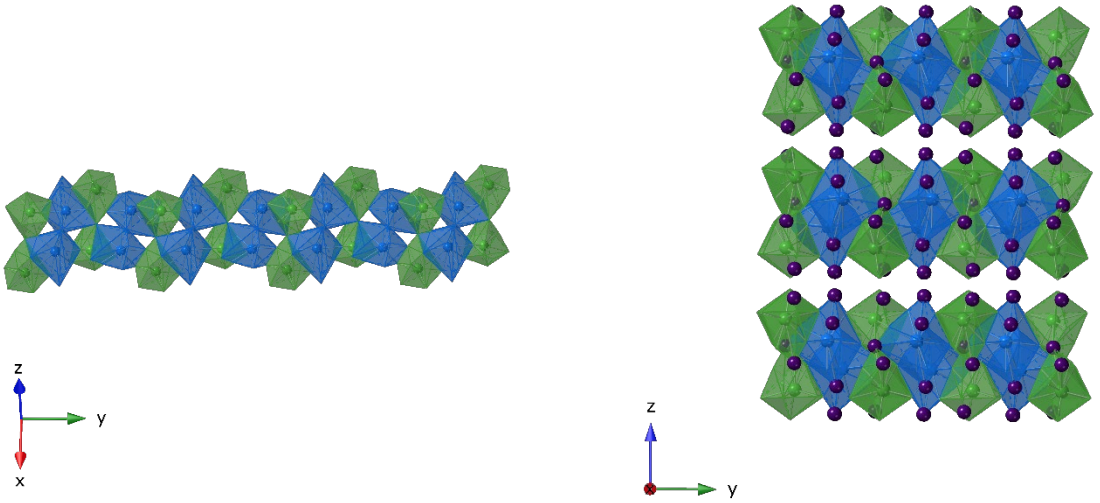

Figure 1. (a) Ball-and-stick representation of $La_2(IO_3)_3(IO_4)$ down the x direction, (b) IO_3, (c) IO_4, (d) LaO_{10}, (e) LaO_9, (f) and (g) Polyhedral views of the structure of $La_2(IO_4)(IO_3)_3$. La in green (ball and stick model) La1 in blue, La2 in green, I in purple, O in red.

Optical Properties

UV−Vis Diffuse Reflectance Spectroscopy

Diffuse reflectance spectra of $La_2(IO_3)_3(IO_4)$ and $Nd_2(IO_3)_3(IO_4)$ were collected using samples consisting of ground crystals and are plotted in Figure 2. As anticipated, due to the absence of f-electrons, no f-f transitions were observed in the spectrum of $La_2(IO_3)_3(IO_4)$. However, the UV−vis absorption spectrum for $Nd_2(IO_3)_3(IO_4)$ consists of many weak absorption bands, as expected for the f−f electronic transitions of the Nd^{3+} ion. The optical band gaps were estimated to be 3.43 and 3.04 eV for $La_2(IO_3)_3(IO_4)$ and $Nd_2(IO_3)_3(IO_4)$, respectively. The estimated band gaps agree well with the observed colors of the compounds, colorless and violet for the La- and Nd-containing compounds, respectively.

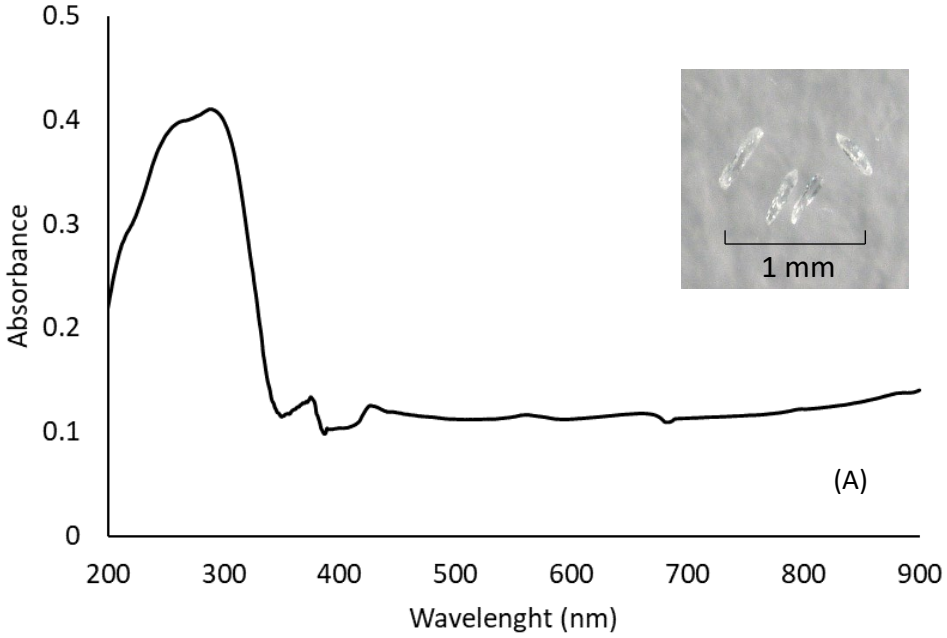
0.5
0.4
0.3
0.2
0.1
0
Absorbance
200
300
400
500
600
700
800
900
Wavelenght (nm)
1 mm
(A)

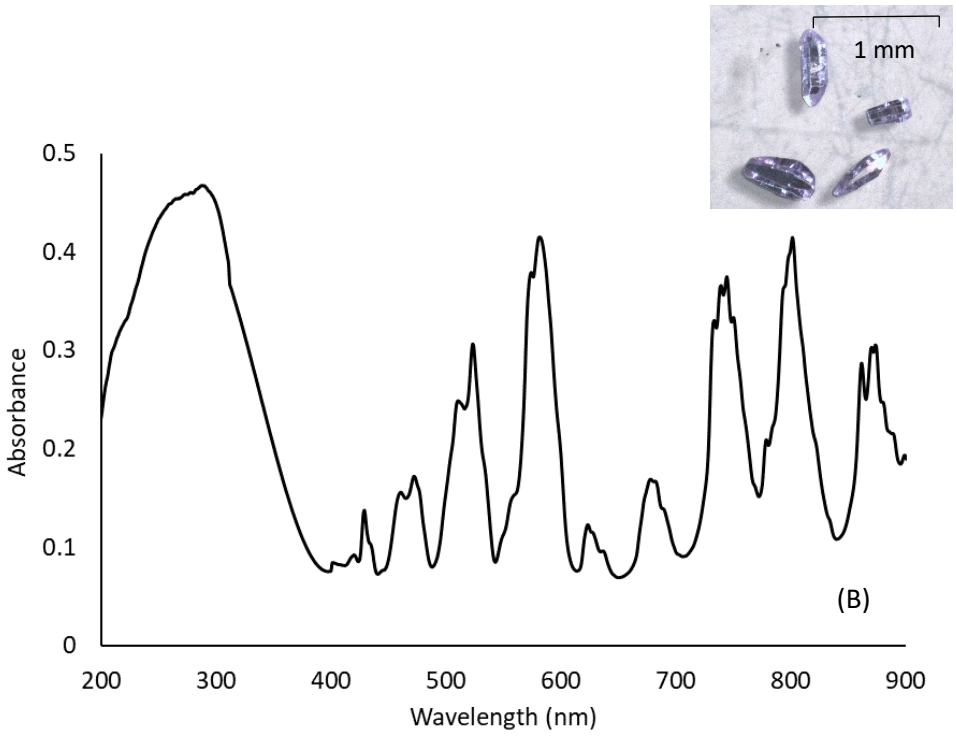

Figure 2. The UV–vis spectrum of $La_2(IO_3)_3(IO_4)$ (A) and $Nd_2(IO_3)_3(IO_4)$ (B).

Luminescence phosphorescence spectra

We investigated the luminescence behavior of the Eu, Tb and Dy doped $La_2(IO_3)_3(IO_4)$ materials. Using the same synthesis procedure that yielded $La_2(IO_3)_3(IO_4)$, we were able to easily introduce 5% Eu, Tb and Dy as dopants into the structure. The structure does not change upon doping. Due to the small doping levels, it was not possible to identify the actual locations, however, the dopant rare earths are assumed to share the lanthanum sites. All three doped materials were found to luminesce. The color of the emitted light, red for Eu-, green for Tb-, and yellow for Dy-doped materials, as expected, is characteristic for the lanthanide dopant used.[17,18]. The emission bands of $La_{1.9}Eu_{0.1}(IO_3)_3(IO_4)$ correspond to the transitions from the lowest excited state, $^5D_0$, to the ground state manifold, ^7F_J (J=6–0) levels of the $4f^6$ configuration.[32] The emission of $La_{1.9}Tb_{0.1}(IO_3)_3(IO_4)$ is due to transitions from the lowest excited state to the ground state, $^5D_4$- ^7F_J (J=6–0). The emission spectra consist of four major emission lines peaking at

around 484, 541, 580 and 619 nm, which are due to the typical $^5D_4 \rightarrow {}^7F_6$, $^5D_4 \rightarrow {}^7F_5$, $^5D_4 \rightarrow {}^7F_4$ and $^5D_4 \rightarrow {}^7F_3$ transitions of the excited Tb^{3+} ions, respectively. The green emission at 545 nm ($^5D_4 \rightarrow {}^7F_5$) is the most intense luminescence emission.[33] The emission of $La_{1.9}Dy_{0.1}(IO_3)_3(IO_4)$ has three $^4F_{9/2} \rightarrow {}^6H_j$ (j = 11/2, 13/2 and 15/2) transitions at 482, 575 and 663 nm, respectively, and the hypersensitive transition is $^4F_{9/2} \rightarrow {}^6H_{13/2}$ with a whitish color which turns to yellow in host lattices.[34,35] Fluorescence emission spectra of $La_2(IO_3)_3(IO_4)$:*Ln* (*Ln*: Eu, Dy, Tb) are plotted in Figure 3. All the characteristic peaks expected of Eu, Dy and Tb are clearly observed.

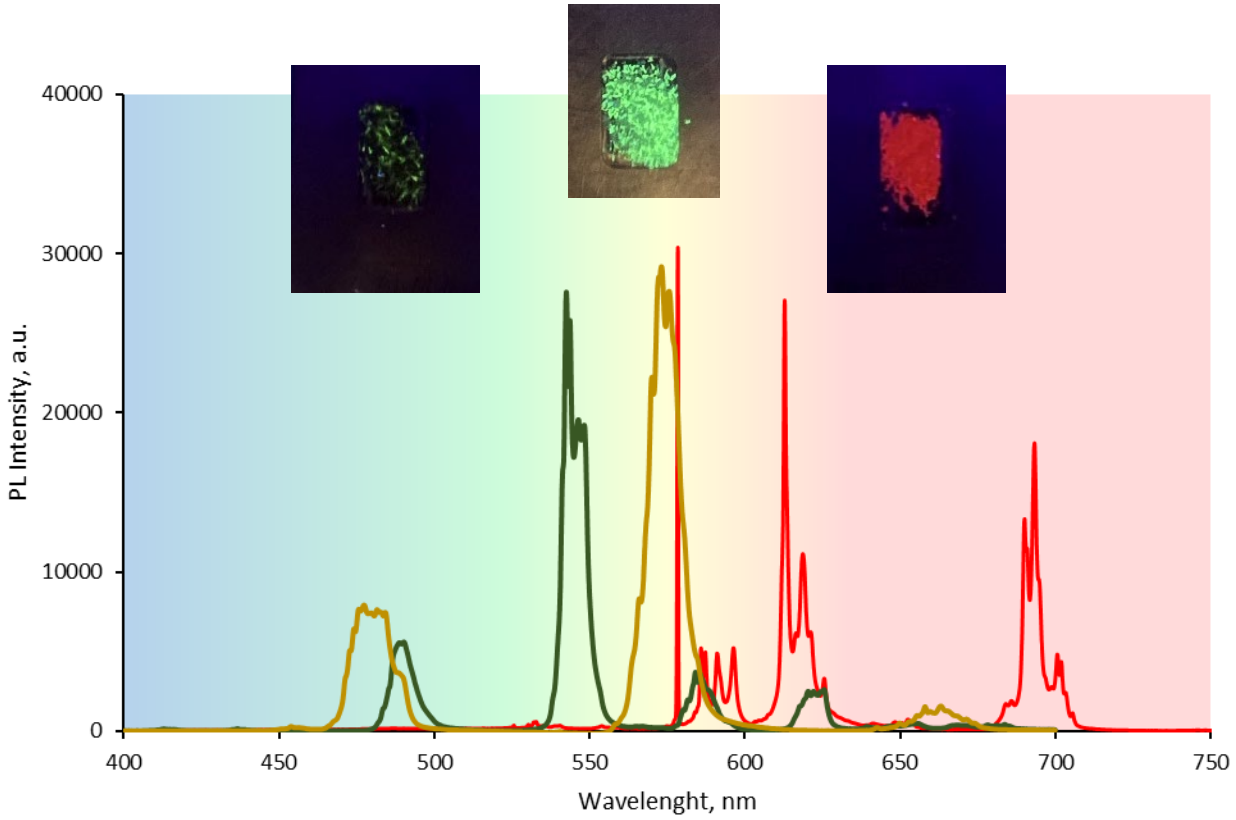

Figure 3. Fluorescence emission spectra (Luminescence spectrum). $La_2(IO_3)_3(IO_4)$:Eu (red), $La_2(IO_3)_3(IO_4)$:Dy (yellow) and $La_2(IO_3)_3(IO_4)$:Tb (green). 375 nm excitation wavelength used.

Figure 4 illustrates the Commission International de I'Eclairage (CIE) chromaticity coordinates of $La_{1.9}Eu_{0.1}(IO_3)_3(IO_4)$, $La_{1.9}Dy_{0.1}(IO_3)_3(IO_4)$, and $La_{1.9}Tb_{0.1}(IO_3)_3(IO_4)$. The CIE chromaticity coordinates (x and y) (Table 2) were computed from the emission spectral profiles

using the color calculator program code (Matlab 7.0 R14). The color purities compared with the 1931 CIE Standard Source.

Table 2. Values of chromaticity coordinates (CIE), correlated color temperatures (CCT, in K) and Yellow/Blue (Y/B) intensity ratios samples at λ_{exc} = 375 nm.

	CIE coordinates			
	x-	**y-**	**CCT**	**Y/B**
$La_{1.9}Tb_{0.1}(IO_3)_3(IO_4)$	0.26	0.73	6486	> 2.5
$La_{1.9}Dy_{0.1}(IO_3)_3(IO_4)$	0.47	0.53	3322	>2.5
$La_{1.9}Eu_{0.1}(IO_3)_3(IO_4)$	0.62	0.38	1889	>2.5

The CCT values computed using McCamy's empirical formula for La $(IO_3)_3(IO_4)$:*Ln.* These CCT values interpreted over the range of 1889-6486 K indicate that the emission color appears almost 'hot' or 'cold', according to the lighting industry convention. Furthermore, the asymmetry ratio (Y/B) calculated. The magnitudes of this ratio (i.e.> 1) express the covalent nature of Ln ions and ligand bond, and also asymmetry around the Ln ions.

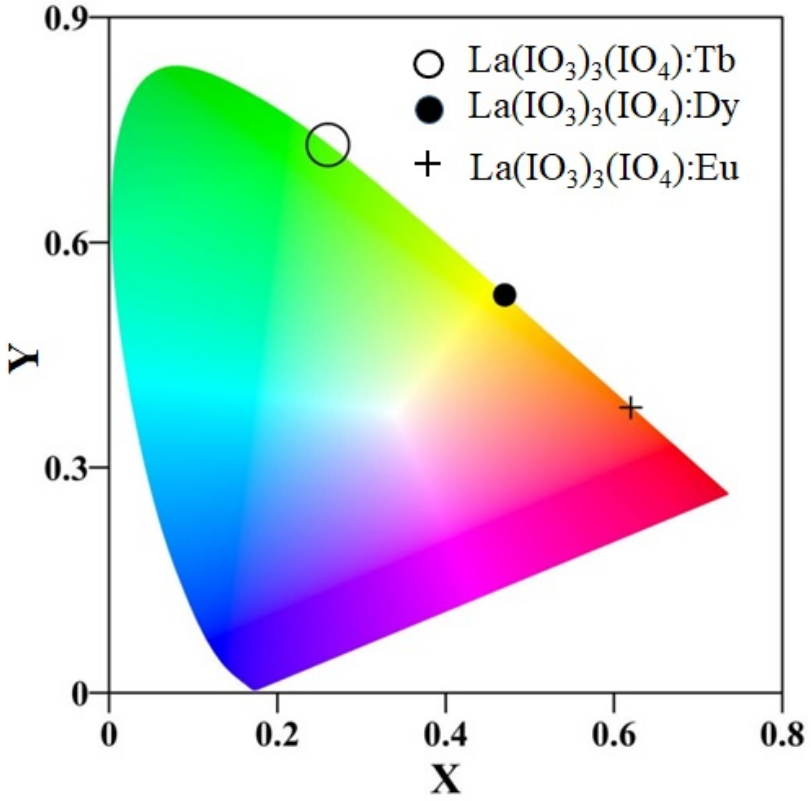

Figure 4. CIE chromaticity diagram at 375 nm excitation.

Conclusions

Crystals of $La_2(IO_3)_3(IO_4)$, $Nd_2(IO_3)_3(IO_4)$ and $Pr_2(IO_3)_3(IO_4)$, grown via a mild hydrothermal route, were found to crystallize in a new structure type that contains isolated $[IO_4]^{3-}$ units. The new framework structures crystallize in the centrosymmetric orthorhombic space group *Pbca*. As the size of lanthanide decreases across the lanthanide series, the stability of the $Ln_2(IO_3)_3(IO_4)$ structure type decreases, resulting to the formation of previously reported $Ln(IO_3)$ composition for *Ln* = Gd, Tb, and Dy. Despite that, $La_2(IO_3)_3(IO_4)$ host matrix was successfully doped with Eu, Tb, and Dy using the same synthetic route and the optical and luminescence properties of all phases were investigated. All the characteristic emission peaks for Eu, Dy and Tb in the doped $La_2(IO_3)_3(IO_4)$ are clearly observed in fluorescence spectra.

Acknowledgements

Financial support for this work was provided by the National Science Foundation under DMR-1806279 and is gratefully acknowledged.

Supporting Information

The Supporting Information is available free of charge at ???

Powder X-ray diffraction patterns, crystallographic tables, SEM images, EDS, BVS, instrumentation used and data collection procedures.

The crystallographic CIF files were deposited into the CCDC data base with CCDC numbers of 2081973-2081975 (https://www.ccdc.cam.ac.uk).

References

1. Hu, C.L.; Mao, J.G. Recent advances on second-order NLO materials based on metal iodates. *Coord. Chem. Rev*. **2015**, *288*, 1-17.

2. Taouti, M.B.; Suffren Y.; Leynaud O.; Benbertal D.; Brenier A.; Gautier-Luneau I. Structures, thermal behaviors, and luminescent properties of anhydrous lanthanum iodate polymorphs. *Inorg. Chem*. **2015**, *54,* 3608-3618.

3. Huang, H.; He, Y.; He, R.; Lin, Z.; Zhang, Y.; Wang, S. Novel Bi-based iodate photocatalysts with high photocatalytic activity. *Inorg. Chem. Commun*. **2014**, *40*, 215-219.

4. Wu, R.; Jiang, X.; Xia, M.; Liu, L.; Wang, X.; Lin, Z.; Chen, C. $K_8Ce_2I_{18}O_{53}$: A novel potassium cerium(IV) iodate with enhanced visible light driven photocatalytic activity resulting from polar zero dimensional $[Ce(IO_3)_8]^{4-}$ units. *Dalton Trans*. **2017**, *46*, 4170-4173.

5. Bean, A.C.; Campana, C.F.; Kwon, O.; Albrecht-Schmitt, T.E. A new oxoanion: $[IO_4]^{3-}$ containing I(V) with a stereochemically active lone-pair in the silver uranyl iodate tetraoxoiodate(V), $Ag_4(UO_2)_4(IO_3)_2(IO_4)_2O_2$. *J. Am. Chem. Soc*. **2001**, *123*, 8806-8810.

6. Sykora, R. E.; Wells, D.M.; Albrecht-Schmitt, T.E. Further evidence for the tetraoxoiodate(V) anion, IO_4^{3-}: Hydrothermal syntheses and structures of $Ba[(MoO_2)_6(IO_4)_2O_4]\bullet H_2O$ and $Ba_3[(MoO_2)_2(IO_6)_2]\bullet 2H_2O$. *Inorg. Chem*. **2002**, *41*, 2697-2703.

7. Mao, F-F.; Hu, C-L.; Chen J.; Wu, B-L.; Mao J-G. $HBa_{2.5}(IO_3)_6(I_2O_5)$ and $HBa(IO_3)(I_4O_{11})$: Explorations of Second-Order Nonlinear Optical Materials in the Alkali-Earth Polyiodate System. *Inorg. Chem*. **2019**, *58*, 3982–3989.

8. Cao, Z.; Yue, Y.; Yao, J.; Lin, Z.; He, R.; Hu, Z. $Bi_2(IO_4)(IO_3)_3$: A new potential infrared nonlinear optical material containing $[IO_4]^{3-}$ anion. *Inorg. Chem*. **2011**, *50*, 12818-12822.

9. Li, Y.; Wu, H.; Zhang, B.; Yang, Z.; Han, G.; Pan, S. Mo^{6+} Cation Enrichment of the Structure Chemistry of Iodates: Syntheses, Structures, and Calculations of $Ba(MoO_2)_2(IO_3)_4O$, $Ba_3[(MoO_2)_2(IO_3)_4O(OH)_4]\bullet 2H_2O$, and $Sr[(MoO_2)_6(IO_4)_2O_4]\bullet H_2O$. *Inorg. Chem*. **2018**, *57*, 9376-9384.

10. Xu, X.; Hu, C.L.; Li, B.X.; Yang, B.P.; Mao, J.G. α-AgI_3O_8 and β-AgI_3O_8 with large SHG responses: Polymerization of IO_3 groups into the I_3O_8 polyiodate anion. *Chem. Mater*. **2014**, *26*, 3219-3230.

11. Tang, C.; Jiang, X.; Yin, W.; Chen, F.; Guo, S.; Song, G.; Liu, L.; Huang, H.; Xia, M.; Lin, Z.; Wang, X. Rubidium Cerium (IV) Iodates with High UV-Light-Driven Photocatalytic Efficiency. *ChemistrySelect*. **2019**, *4*, 7076-7081.

12. Gautier-Luneau, I.; Suffren, Y.; Jamet, H.; Pilmé, J. Reinterpretation of three crystal structures of alkali oxoiodate(v) -description of the $[I_3O_8]^-$ anion and the infinite 2D $[I_3O_8^-]_\infty$ anion. *Z. Anorg. Allg. Chem*. **2010**, *636*, 1368-1379.

13. Tang, C.; Jiang, X.; Guo, S.; Guo, R.; Liu, L.; Xia, M.; Huang, Q.; Lin, Z.; Wang, X.

Synthesis, Crystal Structure, and Optical Properties of the First Alkali Metal Rare-Earth Iodate Fluoride: $Li_2Ce(IO_3)_4F_2$. *Cryst. Growth Des*. **2020**, *20*, 2135-2140.

14. Wibowo, A.; Smith, M.D.; zur Loye, H-C. New 3D bismuth-oxo coordination polymers containing terephthalate-based ligands: Observation of Bi_2O_2-layer and Bi_4O_3-chain motifs. *CrystEngComm*. **2010**, *13*, 426-429.

15. Nguyen, S.D.; Yeon, J.; Kim, S-H.; Halasyamani, P.S. $BiO(IO_3)$: A New Polar Iodate that Exhibits an Aurivillius-Type $(Bi_2O_2)^{2+}$ Layer and a Large SHG Response. *J. Am. Chem. Soc*. **2011**;*133*, 12422–12425.

16. Wibowo, A.C.; Smith, M.D.; Yeon, J.; Halasyamani, P.S.; zur Loye, H-C. Novel 3D bismuth-based coordination polymers: Synthesis, structure, and second harmonic generation properties. *J. Solid State Chem*. **2012**, *195*, 94-100.

17. Binnemans, K. Lanthanide-based luminescent hybrid materials. *Chem. Rev*. **2009**, *109*, 4283-4374.

18. Lis, S. Luminescence spectroscopy of lanthanide(III) ions in solution. *J. Alloys Compd*. **2002**, *341*, 45-50.

19. Eaton, T.; Lin, J.; Cross, J.N.; Stritzinger, J.T.; Albrecht-Schmitt, T.E. $Th(VO_3)_2(SeO_3)$ and $Ln(VO_3)_2(IO_3)$ (Ln = Ce, Pr, Nd, Sm, and Eu): unusual cases of aliovalent substitution. *Chem. Commun*. **2014**, *50*, 3668-3670.

20. Petoud, S.; Cohen, S.M.; Bünzli, J.C.G.; Raymond, K.N. Stable Lanthanide Luminescence Agents Highly Emissive in Aqueous Solution: Multidentate 2-Hydroxyisophthalamide Complexes of Sm^{3+}, Eu^{3+}, Tb^{3+}, Dy^{3+}. *J. Am. Chem. Soc*. **2003**, *125*, 13324-13325.

21. SAINT; Bruker AXS Inc.: Madison, WI, 2012.

22. Krause, L.; Herbst-Irmer, R.; Sheldrick, G.M.; Stalke, D. Comparison of silver and molybdenum microfocus X-ray sources for single-crystal structure determination. *J. Appl. Crystallogr*. **2015**, *48*, 3-10.

23. Dolomanov, O.V.; Bourhis, L.J.; Gildea, R.J.; Howard, J.A.K.; Puschmann, H. OLEX2: A complete structure solution, refinement and analysis program. *J. Appl. Crystallogr*. **2009**, *42*, 339-341.

24. Sheldrick, G.M. Crystal structure refinement with SHELXL. *Acta Crystallogr. Sect C Struct. Chem*. **2015**, *71*, 3-8.

25. Hector, A.L.; Henderson, S.J.; Levason, W.; Webster, M. Hydrothermal Synthesis of Rare Earth Iodates from the Corresponding periodates: Structures of $Sc(IO_3)_3$, $Y(IO_3)_3.2H_2O$, $La(IO_3)_3•1/2H_2O$ and $Lu(IO_3)_3•2H_2O$. *Z. Anorg. Allg. Chem.* **2002**, *628*, 198-202.

26. Douglas, P.; Hector, A.L.; Levason, W.; Light, M.E.; Matthews, M.L.; Webster, M. Hydrothermal synthesis of rare earth iodates from the corresponding periodates: II. Synthesis and structures of $Ln(IO_3)_3$ (Ln = Pr, Nd, Sm, Eu, Gd, Tb, Ho, Er) and $Ln(IO_3)_3.2H_2O$ (Ln = Eu, Gd, Dy, Er, Tm, Yb). *Z.Anorg. Allg. Chemie*. **2004**, *630*, 479-

27. Ok, M.K.; Halasyamani, P.S. New metal iodates: Syntheses, structures, and

characterizations of noncentrosymmetric $La(IO_3)_3$ and $NaYl_4O_{12}$ and centrosymmetric β-$Cs_2I_4O_{11}$ and $Rb_2I_6O_{15}(OH)_2•H_2O$. *Inorg. Chem*. **2005**, *44*, 9353-9359.

28. Klepov, V.V.; Pace, K.A.; Breton, L.S.; Kocevski, V.; Besmann, T.M.; zur Loye, H-C. Nearly Identical but Not Isotypic: Influence of Lanthanide Contraction on $Cs_2NaLn(PS_4)_2$ (Ln=La−Nd, Sm, and Gd−Ho). *Inorg. Chem*. **2020**, *59*, 1905–1916.

29. Klepov, V.V.; Breton, L.S.; Pace K.A.; Kocevski, V., Besmann, T.M.; zur Loye H.-C. Size-Driven Stability of Lanthanide Thiophosphates Grown from an Iodide Flux. *Inorg. Chem*. **2019**, *58*, 6565-6573.

30. Phanon, D.; Gautier-Luneau, I. Promising material for infrared nonlinear optics: NaI_3O_8 salt containing an octaoxotriiodate(V) anion formed from condensation of $[IO_3]^-$ ions. *Angew. Chem., Int. Ed*. **2007**, *46*, 8488-8491.

31. Ok, K.M.; Halasyamani, P.S. The lone-pair cation I^{5+} in a hexagonal tungsten oxide-like framework: Synthesis, structure, and second-harmonic generating properties of $Cs_2I_4O_{11}$. *Angew. Chem., Int. Ed*. **2004**, *43*, 5489-5491.

32. Binnemans, K. Interpretation of europium(III) spectra. *Coord. Chem. Rev*. **2015**, *295*, 1-45.

33. Kotan, Z.; Ayvacikli, M.; Karabulut, Y.; Garcia-Guinea, J.; Tormo, L.; Canimoglu, A.; Karali, T.; Can, N. Solid state synthesis, characterization and optical properties of Tb doped $SrSnO_3$ phosphor. *J. Alloys Compd*. **2013**, *581*, 101-108.

34. Ayvacikli, M.; Ege, A.; Can, N. Radioluminescence of $SrAl_2O_4:Ln^{3+}$ (Ln = Eu, Sm, Dy) phosphor ceramic. *Opt. Mater.* **2011**, *34*, 138-142.

35. Blasse, G.; Grabmaier, B.C. *Luminescent Materials*. Berlin Heidelberg: Springer-Verlag; 1994.

For Table of Contents Use Only

Hydrothermal Synthesis of new Iodates $Ln_2(IO_3)_3(IO_4)$ (*Ln*=La, Nd, Pr) Containing the Tetraoxoiodate(V) Anion: Creation of Luminescence Properties by Doping with Eu, Dy, Tb

Ceren Kutahyali Aslani, Vladislav V. Klepov, Mahmoud A. A. Aslani, and Hans-Conrad zur Loye


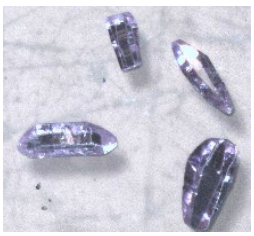
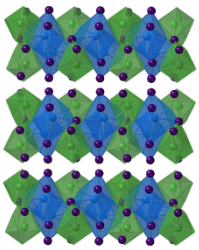

Crystals of $Ln_2(IO_3)_3(IO_4)$ (*Ln*=La, Nd, Pr) that contain isolated $[IO_4]^{3-}$ units were synthesized via a mild hydrothermal route. $La_2(IO_3)_3(IO_4)$ was used as the host matrix for Eu, Tb, and Dy dopants to introduce luminescence.